

IMPROVED PREDICTION OF PROSTATE CANCER RECURRENCE BASED ON AN AUTOMATED TISSUE IMAGE ANALYSIS SYSTEM

Mikhail Teverovskiy¹, Vinay Kumar¹, Junshui Ma¹, Angeliki Kotsianti¹, David Verbel¹, Ali Tabesh^{1,2}, Ho-Yuen Pang¹, Yevgen Vengrenyuk¹, Stephen Fogarasi¹, Olivier Saidi¹

¹Aureon Biosciences Corporation, 28 Wells Ave, Yonkers, NY 10701

²Department of Electrical and Computer Eng., University of Arizona, Tucson, AZ 85721

ABSTRACT

Prostate tissue characteristics play an important role in predicting the recurrence of prostate cancer. Currently, experienced pathologists manually grade these prostate tissues using the Gleason scoring system, a subjective approach which summarizes the overall progression and aggressiveness of the cancer. Using advanced image processing techniques, Aureon Biosciences Corporation has developed a proprietary image analysis system (MAGICTM), which here is specifically applied to prostate tissue analysis and designed to be capable of processing a single prostate tissue Hematoxylin-and-Eosin (H&E) stained image and automatically extracting a variety of raw measurements (spectral, shape, etc.) of histopathological objects along with spatial relationships amongst them. In the context of predicting prostate cancer recurrence, the performance of the image features is comparable to that achieved using the Gleason scoring system. Moreover, an improved prediction rate is observed by combining the Gleason scores with the image features obtained using MAGICTM, suggesting that the image data itself may possess information complementary to that of Gleason scores.

1. INTRODUCTION

Today, pathologists rely on the Gleason scoring system to provide an effective evaluation of how advanced and aggressive a prostate cancer is. It is graded based on the architecture of the prostate tissue as seen under a microscope. The more advanced the cancer is, the higher its Gleason score [1, 2].

Although Gleason grading is widely considered by pathologists to be reliable, it is a subjective scoring system. The pathologist's experience, as well as other factors, can considerably affect the final Gleason scores. Moreover, the Gleason score is categorized into discrete levels to make it easier for pathologists to use.

Meanwhile, new techniques in image processing and analysis have emerged, aided by significantly increased computational power. In many applications, including

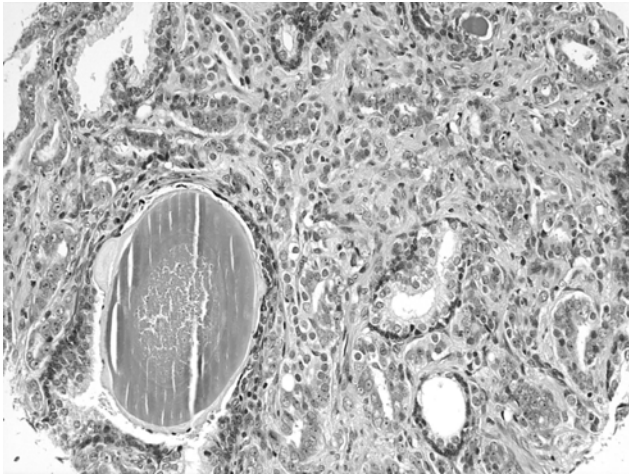
cancer diagnosis and prognosis, the ability to automatically extract large amounts of quantitative continuous-valued features from a single image has become a reality [3, 4]. So far, most cancer image analysis systems have been developed for images taken from cytological specimens, which only capture cells and thus do not utilize all of the architectural information observable at the tissue level [3, 4]. However, the structure of different pathological elements at the tissue level plays a more important role in diagnosis than the appearance of individual cells. For example, in a prostate tissue specimen, the shape and size of the gland are two of the most critical features pathologists use to determine the progression of the cancer [5]. Unfortunately, research on developing practical and high-performance image analysis systems targeting cancer tissues is not widely available in the literature. One reason for the paucity of such research is the difficulty and complexity involved in performing quantitative tissue image analysis. Compared with cellular images, tissue images are more complex and require comprehensive domain expert knowledge to be understood.

MAGICTM is a tissue image analysis system that uses advanced image processing algorithms in order to segment and measure properties of the histopathological objects. In this study, MAGICTM has been used to create an application that takes a prostate tissue H&E image as input and outputs a variety of statistical measurements of histopathological objects present in the image. These extracted features are then used to predict biochemical recurrence in prostate cancer patients who have undergone radical prostatectomy. Both conventional statistical and machine learning methods were utilized. An improved predictive performance is achieved by combining the Gleason scores with a feature vector containing the measurements from MAGICTM.

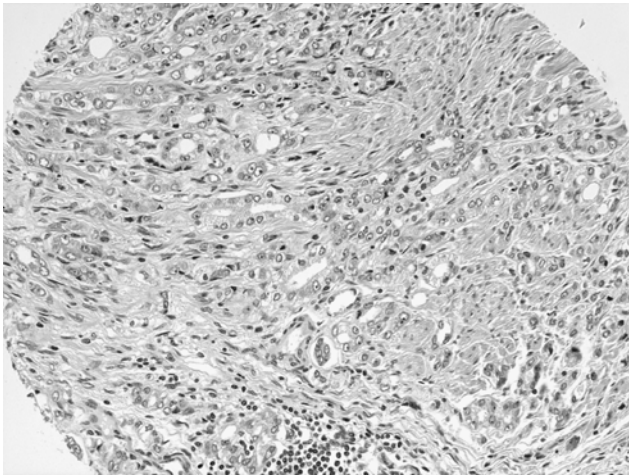
This paper is organized as follows. The complete prostate tissue image analysis application is described in Section 2. In Section 3, the quality of the extracted features is experimentally demonstrated in terms of predicting cancer recurrence. In Section 4, we present the conclusions from our study.

2. PROSTATE TISSUE IMAGE ANALYSIS

MAGIC™'s application for prostate tissue image analysis is an automated, high throughput system capable of analyzing images and producing statistical measurements. The system was developed to analyze H&E stained prostate tissue microarray (TMA) core images. The images are captured by a light microscope at 20X magnification using a SPOT Insight QE Color Digital Camera (KAI2000) producing images with 1600 x 1200 pixels and are stored as 24 bits per pixel images in Tiff format. Examples of normal and abnormal H&E prostate tissue images are shown in Figure 1.



(a) Image of a Healthy Prostate Tissue



(b) Image of an Abnormal Prostate Tissue

Figure 1. H&E Prostate Tissue Image in Grayscale

Initial Segmentation. In MAGIC™ images are first segmented into small groups of contiguous pixels known as objects. These objects are obtained by a region-growing algorithm which finds contiguous regions based on color similarity and shape regularity. The size of the

objects can be varied by adjusting a few parameters [6]. In this system, an object rather than a pixel is the smallest unit of processing. All feature calculations and operations are with respect to objects. For example, when a threshold is applied to the image, the feature values of the object are subject to the threshold. As a result all the pixels within an object are assigned to the same class.

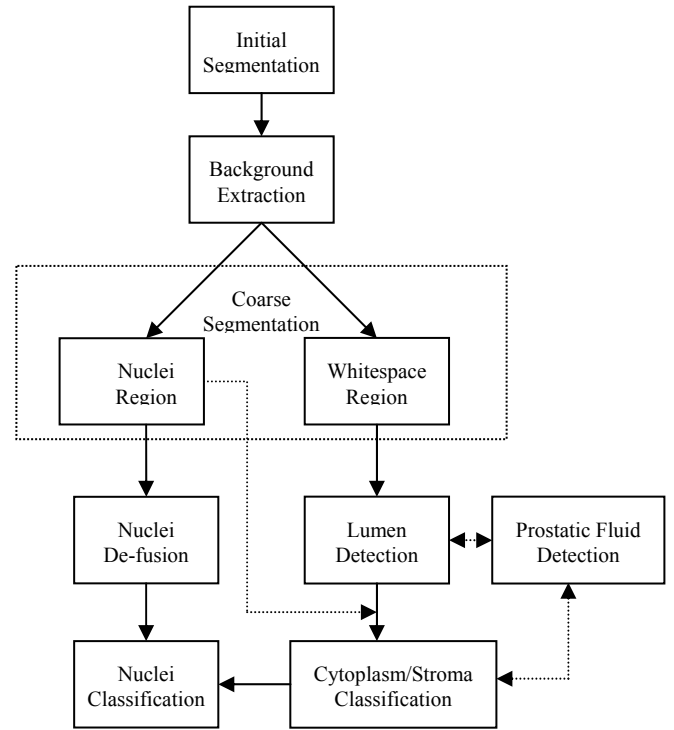


Figure 2. MAGIC™'s application for prostate tissue image analysis

In our application, the size of objects is controlled to be 10-20 pixels at the finest level. Based on this level, subsequent higher and coarser levels are built by forming larger objects from the smaller ones in the lower level. The component modules of the prostate tissue image analysis system are shown as a flow chart in Figure 2.

Background Extraction. The background extraction stage segments the TMA tissue core from the background (transparent region of the slide) using intensity threshold and convex hull.

Coarse Segmentation. The foreground (TMA core) is then re-segmented into rough regions corresponding to nuclei and white spaces. The main characterizing feature of nuclei in H&E stained images is that they are stained blue compared to the rest of the pathological objects. Therefore, the difference in the red and blue channels ($R-B$) is used as a distinguishing feature. The objects which meet the ($R-B$) feature threshold are classified as nuclei area. Similarly, a green channel threshold is used to classify objects in the tissue core as white spaces.

White Space Classification. In the stage of coarse segmentation, the white space regions may correspond to both lumen (pathological object) and artifacts (broken tissue areas) in the image. The smaller white space objects (area less than 100 pixels) are usually artifacts. Area filter is applied to classify them as artifacts.

Nuclei De-fusion and Classification. In the stage of coarse segmentation, the nuclei area is often obtained as contiguous fused regions that encompass several real nuclei. Moreover, the nuclei region might also include surrounding misclassified cytoplasm. These fused nuclei areas need to be de-fused in order to obtain individual nuclei.

Two different approaches have been attempted. The first one is based on a region growing algorithm that fuses the image objects constituting nuclei area under shape constraints (roundness). This approach works well when the fusion is not severe.

In the case of severe fusion, a different approach based on supervised learning has been used. This approach involves manual labeling of the nuclei areas by an expert (pathologist). The features of image objects belonging to the labeled nuclei are used to design statistical classifiers.

In order to reduce the number of feature space dimensions, feature selection was performed on the training set using two different classifiers [7]: the Bayesian classifier and the k nearest neighbor classifier. The leave-one-out method [8] was used for cross-validation, and the sequential forward search algorithm was used to choose the best features. Finally, we designed two Bayesian classifiers with number of features equal to 1 and 5. The class-conditional distributions were assumed to be Gaussian with diagonal covariance matrices.

The input image contains different kinds of nuclei: epithelial nuclei, fibroblasts, basal nuclei, endothelial nuclei, apoptotic nuclei and red blood cells. Since the number of epithelial nuclei is an important feature in grading the extent of the tumor, it is important to distinguish the epithelial nuclei from the others. This is done by classifying the detected nuclei into two classes: epithelial nuclei and “the rest” based on shape (eccentricity) and size (area) features.

Feature Statistics. Once all image objects are correctly classified, they are fused to obtain pathological objects and the various statistical features associated with them are output. They include spectral-based characteristics (channel means, standard deviations, etc.), position, size, perimeter, shape (asymmetry, compactness, elliptic fit, etc.) and relationships to neighboring objects (contrast). These features are produced for every instance of every pathological object in the image. In addition, an overall statistical summary for the image is also output for each of the above mentioned features.

3. PREDICTING PROSTATE CANCER RECURRENCE

The number of raw features extracted from each prostate tissue image using MAGIC™ is initially as large as five hundred. The full set of raw features was chosen agnostically to avoid disregarding potentially useful features. However, these features are not all equally informative. Also a prediction model built based on this full feature set may have poor predictive performance due to the “curse of dimensionality” [8]. So a dimensionality reduction procedure was applied, and a set of eight imaging features was finally selected.

The two questions we would like to now answer are: (1) are these selected raw imaging features indeed useful for prostate cancer prognosis? and (2) do these features provide the same amount of information that has already been provided by those from the Gleason scoring system in terms of predicting prostate cancer recurrence?

To answer these questions, a study was conducted based on a subset of 153 patients from a cohort of prostate cancer patients who underwent radical prostatectomy. Measurable PSA after the operation was used to define prostate cancer recurrence (also referred to as biochemical recurrence). Patients were followed up post-operatively. Their recurrence status at their last visit, as well as their follow-up time, was recorded, which generated a set of right-censored data. Gleason scores were measured both pre-operatively from the biopsy specimen and post-operatively using the excised prostate gland. The four specific measures, or features, considered in this study are (1) the biopsy Gleason grade, (2) the biopsy Gleason score, (3) the post-operative Gleason grade, and (4) the post-operative Gleason score.

In order to answer the first question, we analyzed the image features obtained by MAGIC™ and the Gleason score-based features separately to predict the time to prostate recurrence.

In order to answer the second question, we combined the image and Gleason score features for recurrence time prediction. Improved prediction accuracy achieved by this joint set of features would imply that the image features indeed provide extra information and thus enhances the recurrence prediction rate.

Because this cohort of patients had right-censored outcome data, survival analysis models had to be built for the prediction of recurrence. In order to avoid the potential algorithmic bias on different types of data, two survival analysis algorithms were used: 1) a Cox regression model [9]; and 2) an Aureon-developed model called Support Vector Regression for censored data (SVRc) adapted from support vector machines [10]. The concordance index estimated using 5-fold cross validation was used to measure the models’ predictive accuracy [8, 11].

Both algorithms were applied to three data sets: (1) the Gleason score features alone; (2) the selected image features alone; and (3) the combination of the image features and the Gleason score features. The experimental results are listed in Table 1.

	Gleason	Image	Gleason + Image
Cox	0.6952	0.6373	0.7261
SVRc	0.6907	0.7269	0.7871

Table 1 - Comparison of Prediction Accuracy

Both questions raised at the beginning of this section are answered by these experimental results. According to Table 1, the predictive performance of the image features are comparable with that of the Gleason scores, and the combination of the image features and the Gleason scores achieves a higher predictive rate, which confirms that the image features extracted by the MAGIC™ system indeed provide extra information beyond the Gleason scores. Therefore the use of the image measurements can enhance the overall recurrence prediction.

4. CONCLUSION

The MAGIC™ image analysis system developed by Aureon Biosciences Corporation enables the processing of prostate H&E tissue images, i.e., segmenting into pathologically valid objects and measuring their properties. The feature vector formed from a subset of the measurements is capable of enhancing the accuracy of predicting prostate cancer recurrence. Statistical modeling based on the measured data showed that the extracted image features provide complementary information to the existing Gleason scoring system.

Future work in this area will include applying the current methodology to other kinds of tissues (breast, liver, etc.) and extending the system within prostate cancer to be able to predict the Gleason score itself from the image features, creating a fully automated system for prostate cancer prognosis.

ACKNOWLEDGMENTS

The authors would like to acknowledge the help and support of Jon Edelson, M.D., Carlos Cordon-Cardo, M.D., Ph.D., Raju Datla, Seetha Datla, and our other colleagues at Aureon Biosciences Corporation.

5. REFERENCES

[1] Scherr D., Swindle P.W. and Scardino P.T., "National Comprehensive Cancer Network Guidelines for the Management of Prostate Cancer," *Urology* 61 (2 Suppl 1): 14-24, Feb. 2003.

[2] Swindle P.W., Kattan M.W. and Scardino P.T., "Markers and Meaning of Primary Treatment Failure," *Urologic Clinics of North America*. 30(2):377-401, May 2003.

[3] Wahlby C., Lindblad J., Vondrus M., Bengtsson E. and Bjorkesten L., "Algorithms for Cytoplasm Segmentation of Fluorescence Labeled Cells," *Analytical Cellular Pathology* 24, 101-111, 2002.

[4] Street W.N., "Xcyt: A System for Remote Cytological Diagnosis and Prognosis of Breast Cancer," In *Soft Computing Techniques in Breast Cancer Prognosis and Diagnosis*, L.C. Jain (ed.), CRC Press, 1999.

[5] Gleason D.F., "The Veteran's Administration Cooperative Urologic Research Group: Histologic Grading and Clinical Staging of Prostatic Carcinoma," In *Urologic Pathology: The Prostate*, Tannenbaum M. (ed.), 171-198, Lea and Febiger, Philadelphia, 1977.

[6] Baatz M. and Schäpe A., "Multiresolution Segmentation – An Optimization Approach for High Quality Multi-scale Image Segmentation," In *Angewandte Geographische Informationsverarbeitung XII*, Strobl, J., Blaschke, T., Griesebner, G. (eds.), Wichmann-Verlag, Heidelberg, 12-23, 2000.

[7] Fukunaga K., *Introduction to Statistical Pattern Recognition*, 2nd Edition, Boston: Academic Press, 1990.

[8] Duda R.O., Hart P.E. and Stork D.G., *Pattern Classification*, 2nd Edition, John Wiley & Sons Inc., 2001.

[9] Cox D.R., "Regression Models and Life Tables," *Journal of the Royal Statistical Society B* 34, 187-220, 1972.

[10] Scholkopf C., Burges C. and Smola A., *Advances in Kernel Methods: Support Vector Learning*, MIT Press, Cambridge, 1999.

[11] Harrell F.E., *Regression Modeling Strategies*, Springer-Verlag 2001.